Multiple Equilibria Analyses of Gas−Porous Solid Isotherms

Russell S. Drago,* Wm. Scott Kassel, Douglas S. Burns,† J. Michael McGilvray, Steven K. Showalter,‡ and Todd J. Lafrenz§

Catalysis Center, Department of Chemistry, University of Florida, Gainesville, Florida 32611

Received: May 1, 1997⊗

This article confirms the physical significance of a new method for determining adsorption energy distributions in porous materials. The premise of the model is that an adsorption isotherm consists of several equilibrium processes corresponding to adsorption into a distinct pore size regime. A distribution type equilibrium constant, *K*, involving the gas and adsorbate in a pore of capacity *n* describes each process. In order to define the *n*'s and *K*'s for all the processes involved, isotherms are collected at several temperatures to minimize the ratio of unknowns to knowns. In this article the model is extended to a series of adsorptives and it is shown that the resulting *K*'s, ΔH's, and *n*'s are not meaningless empirical fit parameters but have the meaning suggested by the model. The ΔG's vary linearly with ΔH for each pore size regime and both correlate linearly with the square root of the van der Waals *a* parameter, $a^{1/2}$. In addition to providing strong support for the physical significance of the parameters, these correlations enable prediction of the *K* values for adsorption of a new adsorptive by a characterized adsorbent given the *a* parameter of the adsorptive. The correlations show that the strongest binding corresponds to the adsorptive selecting pores from the distribution available that match its molecular dimensions. The *n*'s for the different adsorptives provide insight into the pore distribution in the solid and about the pores utilized in the adsorption of different adsorptives. Prediction of the *K*'s from *a* and estimating *n*'s from molecular diameters is suggested as a way to attain the long-range goal of predicting the total isotherm for a new adsorptive from molecular properties. The practical application of this information for use in separations is illustrated. The concept of effective pressure, P_{eff}, is introduced for catalysis to allow comparison of the concentrating effect of different microporous solids.

Introduction

Adsorption isotherms provide a quantitative measure of the heterogeneous equilibria involved in the adsorption of a gas by a solid. A generalized description of heterogeneous equilibria uses the Langmuir equation which can be derived from kinetic, thermodynamic, or statistical mechanical considerations.[1,2] In the kinetic model, the rate of adsorption depends on the fraction of the surface that is bare, while evaporation depends on the fraction of the surface covered. At equilibrium, these rates are equal leading to the following expression for adsorption on a plane surface.

$$\frac{N_A}{N_0} n = \frac{\sigma\mu}{1 + \sigma\mu} \tag{1}$$

In this equation, N_A is Avogadro's number, N_0 is the number of adsorption sites on the surface of the solid, *n* is the amount adsorbed, σ is related to the fraction of the gas molecules adsorbed and to the evaporation rate, and μ is proportional to the equilibrium pressure of the adsorptive and to the temperature. This model assumes that all of the adsorption sites are equivalent and that each site only contains a single molecule that does not interact with any neighboring molecules. Provisions were made for more than one kind of adsorption site.[1] In this case, reactions on different types of surface sites make different contributions to the chemical equilibrium. If B_i is the fraction of the adsorption due to site type *i*, and there are *i* different types of sites, eq 1 becomes

$$\frac{N_A}{N_0} n = \sum_i \frac{B_i \sigma_i \mu}{1 + \sigma_i \mu} \tag{2}$$

Because of the structural and surface heterogeneity of microporous materials, such as activated carbon, a multitude of sites are anticipated and the Langmuir model has not been used.[3−7] Various approaches have been employed to account for heterogeneities. Many have focused on the estimation of adsorption potential energy distributions.[8−11] Some assume a Gaussian energy or size distribution of the micropores. This includes the classic Dubinin−Radushkevich (DR) approach which is found to be an approximate form of an isotherm derived from statistical mechanical principles by Yang.[12] The Gibbs' energy distribution of the micropores has also been used in place of the Gaussian assumption[9] as have other model equations.[13] Ross and Morrison[14] assumed that the surface of the adsorbent is composed of many different unisorptic patches, each with a unique adsorption potential that is systematically adjusted to fit the isotherm. While all of these methods fit experimental adsorption isotherms, they are lacking in their descriptions of the influence of adsorptive and adsorbent physical properties on adsorption.

Everett and Powl have calculated potential energies for adsorption by slitlike pores.[15] The maximum enhancement in the energy of adsorption for these types of pores, compared to adsorption on a graphite plane surface, occurs when the walls of the pore are separated by a distance corresponding to the molecular diameter of the adsorptive. Adsorption approached that on a graphitic plane when the width of the pore is two adsorptive diameters. This suggests that the energy of adsorp-

* Corresponding author. Tel.: (904) 392-6043. Fax: (904) 392-4658.
† ENSCO Inc. 445 Pineda Ct., Melbourne, FL 32940.
‡ Division 6216, P.O. Box 5800, MS0703, Sandia National Labs, Albuquerque, NM 86185-0703.
§ University of Nevada−Reno, C.E.S.E., Mailstop 199, Reno, NV 89557.
⊗ Abstract published in *Advance ACS Abstracts,* August 15, 1997.

S1089-5647(97)01490-9 CCC: $14.00

tion for a given microporous material is determined by the size of the adsorbing pore relative to the site of the adsorptive.

A recent contribution from this laboratory introduced a new method to account for the heterogeneity of microporous carbons.[16] The model is based on a multiple equlibrium description of the isotherm and makes no assumptions with respect to adsorption by specific surface sites or to an adsorption energy distribution. Instead, adsorption processes are determined by a series of *distribution* type equilibria involving pores with different widths relative to the molecular diameter of the adsorptive. The equilibria are expressed by eq 3.

$$\mathrm{SA} = \sum_{i} \frac{n_i K_i P_{\mathrm{equil}}}{1 + K_i P_{\mathrm{equil}}} \qquad (3)$$

In this equation, SA is the amount of gas adsorbed in mol·g^{-1}, i is the minimum number of processes necessary to fit the data as accurately as they are known, n_i is the capacity for process i in mol·g^{-1}, K_i is an equilibrium constant describing adsorption process i, and P_{equil} is the equilibrium pressure of the adsorptive in atmospheres. A given K value may include groups of processes whose individual K_i's are so similar that experimental precision does not allow their resolution. *Therefore, each K_i may be considered as an average value that covers a narrow range of pore sizes.*

Equation 3 is similar in form to the Langmuir equation but is conceptually very different. *The emphasis on sites is replaced by accessible pore volumes available for each of the individual processes.* With this in mind, the equilibrium constants for physisorption are in effect distribution coefficients involving the gaseous adsorptive in equilibrium with condensed molecules within the pores of the solid. The pores with molecular dimensions fill first with several processes occurring simultaneously. *Neighbor interactions are expected as surface coverage progresses.* From this point forward, the term *process* will be used to describe adsorption occurring within a specific pore size regime as opposed to adsorption by a specific surface site.

Another important feature of the multiple equilibrium, analysis, MEA, is the *measurement of isotherms at several temperatures.* In the case of a three-process system, i.e., three average pore size regimes for a given adsorptive, solving for the resulting six unknown K's and n's in eq 3, using a single experimental isotherm leads to a shallow minimum in the data fit and uncertainty in the parameters. A better minimum can be reached by collecting isotherms at a series of different temperatures and solving all of the resulting data sets simultaneously. The only new unknowns added to the system for each new temperature are the new sets of K's. The n values, like solid and liquid densities are, for practical purposes, temperature independent as they represent the solids maximum capacity for each process and, as such, the same set applies for a given adsorptive−adsorbent system at the different temperatures. Using the three-process example above, the 6:1 ratio of unknowns to isotherms becomes 9:2 for two isotherms, 12:3 for three, 15:4 for four, etc. The higher ratio of experimental isotherms to unknowns leads to a better definition of the minimum in the analysis of the combined data set.

In the first article of this series, adsorption by two microporous carbonaceous adsorbents[16] were fit to three processes that were interpreted as adsorption on the surfaces of the very small micropores, $i = 1$, adsorption on the surfaces of larger micropores, $i = 2$, and adsorption and multilayer formation on the surface of the remaining micropores and solid surface, $i = 3$. As with all of the current methods available for the analysis of adsorption data, the multiple equilibrium model relies on and produces an excellent empirical fit of the experimental data. However, a new model will be significant only if the resulting parameters obtained from the fit of different adsorptives and adsorbents have meaning within the context of the model and offer new insights concerning the adsorption process. The direct thermodynamic basis for the parameters of the multiple equilibrium model have these advantages if it can be demonstrated that the data fit provides meaningful results. To accomplish this objective more test cases are needed.

The expanded set of adsorptives used in this article includes larger adsorptive molecules, CH_4, C_2H_6, and C_3H_8. The $-\Delta G$ and $-\Delta H$ values for adsorption will be shown to correlate to molecular properties of the adsorptives. This leads to a characterization of the dispersion characteristics of the adsorbents. These correlations indicate that the parameters obtained from the data fits have the thermodynamic meaning implied by the model employed. Furthermore, a long-range goal of isotherm modeling is the prediction of adsorption isotherms from fundamental properties. The potential use of the MEA model to predict isotherms is discussed.

The process capacities, n_i's, are used with the adsorptives' molar volumes to provide accessible pore volumes for different adsorptives that can be contrasted to those determined from conventional N_2 porosimetry methods. In addition, these capacities and the adsorptive cross-sectional areas can be used to calculate accessible surface areas for different size adsorptives for each resolved process. These areas are contrasted to the N_2 BET areas which are known to be fraught with difficulties for porous solids.

Experimental Section

Adsorbents and Adsorptives. The carbonaceous adsorbents used in this study are Ambersorb 572, A572, and PPAN. These adsorbents are made via the controlled pyrolysis of precursor resins: a polysulfonated polystyrene resin in the case of A572 and poly(acrylnitrile) for PPAN. Rohm and Haas Co. provided both adsorbents.

The adsorbents were characterized using C, H, and N analyses and standard porosimetry techniques. Surface area and pore volume data were obtained from N_2 isotherms taken at 77 K using a Micromeritics ASAP 2000 system. The surface areas were determined using a five-point BET,[17] (Brunauer−Emmett−Teller) calculation while the micropore volumes were calculated with the Harkins−Jura[18] *t*-plot method using thickness parameters from 5.5 to 9.0 Å. The BJH,[19] (Barrett−Joyner−Halenda) adsorption curve was used for calculating meso− and macropore volumes. A572 and PPAN have BET surface areas of 1160 and 880 m^2 g^{-1}, respectively. The micro-, meso-, and macropore volumes are 0.43, 0.28, and 0.21 mL g^{-1} for A572, and 0.33, 0.13, and 0.09 mL g^{-1} for PPAN. C, H, and N analyses were performed by the University of Florida elemental analysis laboratory and are as follows: A572 C = 91%, H = 0.3%, and N = 0%; PPAN C = 70%, H = 1.5%, and N = 5.0%.

He and N_2, 99.99% purity, were obtained from Liquid Air, Inc. CO, CO_2, CH_4, C_2H_6, and C_3H_8 were purchased from Matheson Gas Co. All gases were used without further purification.

Adsorption Measurements. All of the reported adsorption data was collected using a Micromeritics ASAP 2000 chemi system. Pressure measurements were made using 1000 and 10 Torr pressure transducers with resolutions of 0.052 and 0.0005 Torr, respectively. Approximately 0.3 g of the adsorbent were used for each experiment. The sample was degassed at 200 °C under vacuum of $<10^{-3}$ Torr for at least 8 h prior to the collection of data. Each experiment consisted of the collection

TABLE 1: Summary of Adsorptives and Their Physical Properties[a]

adsorptive	MW (g/mol)	polarizability[b] (A^3)	van der Waals *a*	dipole moment[c] (D)	molar vol[d] (mL/mol)	T_c (°C)	T_b (°C)	ΔH_v (kcal/mol)
He	4.00	0.205	0.03412	0	32.0	−268.0	−268.9	0.0194
N_2	28.01	1.74	1.390	0	35.4	−146.9	−195.8	1.33
CO	28.01	1.95	1.485	0.13	34.9	−140.2	−191.5	1.44
CH_4	16.04	2.59	2.253	0	37.8	−82.6	−161.5	1.95
C_2H_6	30.07	4.47	5.489	0	52.6	32.3	−88.65	3.52
C_3H_8	44.10	6.29	8.664	0.084	75.0	96.7	−42.1	4.49

[a] *Lange's Handbook of Chemistry*, 13th ed.; McGraw-Hill: New York, 1985. All data from this source unless otherwise specified. [b] *Handbook of Chemistry and Physics*, 71st ed.; CRC Press: Boca Raton, FL, 1991. [c] McClellan, A. L. *Tables of Experimental Dipole Moments*; W. H. Freeman & Co.: San Francisco, 1963; p 123. [d] Molar volume of the liquid at the normal boiling point. Hildebrand, J. H.; Prausnitz, J. M.; Scott, R. L. *Regular and Related Solutions*; Von Nostrand Reinhold Co.: New York, 1970; p 217. [e] McClellan, A. L.; Harnsberger, H. F. *J. Colloid Interface Sci.* **1967**, *23*, 577.

of 36−50 adsorption points covering a pressure range from 1 to 760 Torr. The majority of the points were taken below 100 Torr. Temperatures below ambient were maintained using an appropriate solvent−liquid nitrogen, or dry ice, slurry.[20] Elevated temperatures were maintained with the heating mantle/thermocouple unit provided with the instrument. All temperatures were held to within 1 °C of the reported temperature.

Data Analysis. Fitting of the collected data to the multiple equilibrium model is accomplished through a series of steps. The raw adsorption data is in the form of volume adsorbed in cm^3/g at STP and equilibrium pressure in Torr. This is converted to moles adsorbed per gram by dividing by 22 414 $cm^3 \cdot mol^{-1}$ gas and to equilibrium pressure in atmospheres by dividing by 760 Torr. A plot of $P_{equil} \cdot mol^{-1}$ adsorbed vs P_{equil} is constructed for each temperature set. Each isotherm is then divided into several straight-line regions, generally three for carbons and two for zeolites and porous silicas. An initial estimate of n is calculated from the slope of the line and K from the intercept in each region. The slope and intercept are determined from a linear regression of the points in that region. The lowest pressure region is associated with process 1; the next with process 2, continuing until the estimated number of straight-line regions is used to fit the entire isotherm.

Only one set of n values is needed for the fit since the n's are temperature independent. The initial value of n_3 is taken from the temperature set closest to the critical temperature of the adsorptive. The value for n_2 is taken from either the same temperature set or the next highest, and n_1 from the highest temperature set. At these temperatures each quantity is the best defined. The only purpose of this procedure is to obtain initial parameter guesses which consist of one set of n values and a set of K values for each temperature. The data are then fit with a nonlinear least-squares method employing a modified simplex routine.[21,22] For the initial fit, each parameter is given a 10% bound and all of the temperature sets for a specific probe are fit simultaneously. In successive fits, the bound is reduced to 1% of the parameter. The parameters obtained from the initial fit are then entered as the initial parameters for the next fit. The parameters from the second fit are then entered into the third fit and each successive fit is done accordingly. This procedure is used since several local minima are found during the first few fits and, therefore, the fitting process is not assumed to be complete until *all* of the parameters cease to vary from fit to fit.

Results and Discussion

The research presented employs two chemically different carbonaceous adsorbents: Ambersorb 572, A572, which is made by the pyrolysis of sulfonated, macroreticular polystyrene beads, and PPAN, a pyrolyzed poly(acrylnitrile) material.[23−26] Each has a large BET surface area and a pore distribution that includes micro-, meso-, and macropores. The main difference between the two materials is the residual N-donor functionality that is present in PPAN.

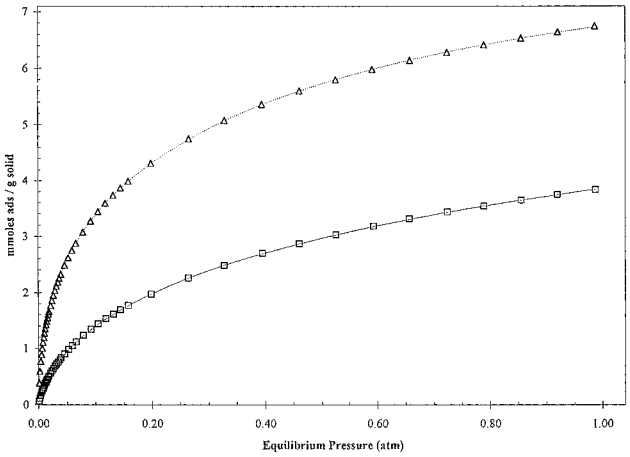

Figure 1. Isotherms for the adsorption of CO and CH_4 by A572 at −77 °C. Points represent experimental adsorption values, □ for CO adsorption, and △ for CH_4 adsorption, while the solid and dashed lines represent the calculated isotherms, for CO and CH_4 respectively, using the n and K values in Table 2 with eq 3.

The adsorptives used, listed in Table 1 along with some of their physical properties, were chosen to encompass a range of polarizability and size. Helium is used as a reference point to determine the dead volume of each adsorbent. N_2, CO, CH_4, and C_2H_6 adsorption equilibrium measurements were taken above each adsorptive's critical temperature to prevent the possibility of capillary condensation and reduce possible contributions from multilayer adsorbate−adsorbate interactions. The adsorptives studied cover a range of physical properties that will allow for the comparison of the dispersive properties of the selected adsorbents.

Figure 1 shows typical adsorption isotherms for CO at −77 °C and CH_4 at −77 °C on A-572. The points correspond to experimental adsorption while the solid lines are generated using the n_i's and K_i's determined from the data fit and eq 3, vide infra. Type 1 isotherms were observed for all of the adsorptives at the temperatures and pressures studied.[3]

Analysis of the Adsorption Isotherms. The parameters from the multiple equilibrium analysis of the measured isotherms are given in Table 2. The previous adsorption parameters[16] for N_2 and CO have been improved by the simultaneous fitting procedure described above. The process capacities, n_i, reflect the number of moles of adsorptive that can be adsorbed by pores with a specific width or range of widths. The equilibrium

TABLE 2: Equilibrium Constants, *n* Values,[a] Enthalpies,[b] and Free Energies[c]

N_2/A572

	$n_1 = 0.463 \pm 0.006$ $-\Delta H_1 = 4.80 \pm 0.01$		$n_2 = 1.79 \pm 0.04$ $-\Delta H_2 = 4.3 \pm 0.2$		$n_3 = 5.3 \pm 0.2$ $-\Delta H_3 = 3.0 \pm 0.2$	
T (°C)	K_1	$-\Delta G_1$	K_2	$-\Delta G_2$	K_3	$-\Delta G_3$
−93	88.15 ± 0.02	1.6022	8.626 ± 0.005	0.7708	0.752 ± 0.001	−0.102
−43	4.5 ± 0.1	0.69	0.72 ± 0.03	−0.15	0.111 ± 0.009	−1.004
0	0.922 ± 0.002	−0.0441	0.1379 ± 0.0006	−1.0747	0.0457 ± 0.0002	−1.674

N_2/PPAN

	$n_1 = 0.50 \pm 0.01$ $-\Delta H_1 = 4.8 \pm 0.1$		$n_2 = 1.59 \pm 0.09$ $-\Delta H_2 = 4.4 \pm 0.3$		$n_3 = 3.6 \pm 0.2$ $-\Delta H_3 = 2.70 \pm 0.1$	
T (°C)	K_1	$-\Delta G_1$	K_2	$-\Delta G_2$	K_3	$-\Delta G_3$
−93	84.65 ± 0.02	1.5877	8.723 ± 0.007	0.7748	0.813 ± 0.003	−0.0739
−43	4.21 ± 0.08	0.657	0.66 ± 0.03	−0.19	0.12 ± 0.01	−0.98
25	0.46 ± 0.01	−0.46	0.043 ± 0.004	−1.86	0.042 ± 0.002	−1.87

CO/A572

	$n_1 = 0.52 \pm 0.01$ $-\Delta H_1 = 5.3 \pm 0.3$		$n_2 = 1.90 \pm 0.09$ $-\Delta H_2 = 4.3 \pm 0.3$		$n_3 = 4.9 \pm 0.9$ $-\Delta H_3 = 3.4 \pm 0.2$	
T (°C)	K_1	$-\Delta G_1$	K_2	$-\Delta G_2$	K_3	$-\Delta G_3$
−93	249 ± 2	1.9740	19.8 ± 0.5	1.0690	1.4 ± 0.2	0.110
−77	60 ± 2	1.60	5.8 ± 0.4	0.69	0.5 ± 0.2	−0.200
−62	26.4 ± 0.6	1.372	3.1 ± 0.2	0.4800	0.34 ± 0.06	−0.460
−43	9.7 ± 0.61	1.03	1.37 ± 0.03	0.1450	0.16 ± 0.01	−0.820

CO/PPAN

	$n_1 = 0.57 \pm 0.02$ $-\Delta H_1 = 5.36 \pm 0.09$		$n_2 = 1.8 \pm 0.2$ $-\Delta H_2 = 4.9 \pm 0.3$		$n_3 = 3.6 \pm 0.7$ $-\Delta H_3 = 2.9 \pm 0.3$	
T (°C)	K_1	$-\Delta G_1$	K_2	$-\Delta G_2$	K_3	$-\Delta G_3$
−93	243 ± 1	1.965	18.7 ± 0.5	1.048	1.3 ± 0.2	0.10
−43	8.8 ± 0.3	0.99	1.10 ± 0.08	0.0452	0.15 ± 0.04	−0.88
25	0.70 ± 0.03	−0.21	0.05 ± 0.01	−1.8	0.050 ± 0.005	−1.78

CH_4/A572

	$n_1 = 0.94 \pm 0.01$ $-\Delta H_1 = 6.2 \pm 0.4$		$n_2 = 2.5 \pm 0.1$ $-\Delta H_2 = 5.1 \pm 0.2$		$n_3 = 5 \pm 1$ $-\Delta H_3 = 4.0 \pm 0.3$	
T (°C)	K_1	$-\Delta G_1$	K_2	$-\Delta G_2$	K_3	$-\Delta G_3$
−77	359.6 ± 0.6	2.2922	20.1 ± 0.2	1.168	1.8 ± 0.1	0.22
−62	100 ± 2	1.93	7.9 ± 0.6	0.87	0.8 ± 0.3	−0.07
−43	23.7 ± 0.2	1.447	2.41 ± 0.07	0.402	0.30 ± 0.03	−0.55
0	4.10 ± 0.01	0.766	0.505 ± 0.004	−0.370	0.103 ± 0.002	−1.235

CH_4/PPAN

	$n_1 = 0.29 \pm 0.01$ $-\Delta H_1 = 6.81 \pm 0.06$		$n_2 = 1.40 \pm 0.05$ $-\Delta H_2 = 5.59 \pm 0.01$		$n_3 = 3.6 \pm 0.3$ $-\Delta H_3 = 4.70 \pm 0.03$	
T (°C)	K_1	$-\Delta G_1$	K_2	$-\Delta G_2$	K_3	$-\Delta G_3$
−43	91.2 ± 0.1	2.063	9.98 ± 0.02	1.051	0.933 ± 0.007	−0.0316
0	8.6 ± 0.1	1.17	1.46 ± 0.02	0.204	0.186 ± 0.009	−0.912
25	2.9 ± 0.1	0.64	0.60 ± 0.03	−0.30	0.09 ± 0.01	−1.5
40	1.93 ± 0.08	0.409	0.39 ± 0.02	−0.58	0.061 ± 0.007	−1.74

C_3H_8/A572

	$n_1 = 0.198 \pm 0.003$ $-\Delta H_1 = 12 \pm 3$		$n_2 = 1.01 \pm 0.01$ $-\Delta H_2 = 9.4 \pm 0.3$		$n_3 = 2.5 \pm 0.1$ $-\Delta H_3 = 8.3 \pm 0.6$	
T (°C)	K_1	$-\Delta G_1$	K_2	$-\Delta G_2$	K_3	$-\Delta G_3$
125	118.8 ± 0.7	3.7787	13.4 ± 0.1	2.050	1.20 ± 0.05	0.145
150	29.5 ± 0.4	2.844	6.80 ± 0.07	1.611	0.68 ± 0.03	−0.32
175	23.3 ± 0.2	2.802	3.52 ± 0.05	1.120	0.37 ± 0.02	−0.90

C_3H_8/PPAN

	$n_1 = 0.221 \pm 0.004$ $-\Delta H_1 = 12.6 \pm 0.3$		$n_2 = 0.87 \pm 0.02$ $-\Delta H_2 = 9 \pm 1$		$n_3 = 1.5 \pm 0.1$ $-\Delta H_3 = 8 \pm 2$	
T (°C)	K_1	$-\Delta G_1$	K_2	$-\Delta G_2$	K_3	$-\Delta G_3$
125	86.1 ± 0.7	3.524	9.4 ± 0.2	1.77	1.2 ± 0.1	0.15
150	33.0 ± 0.2	2.940	5.26 ± 0.06	1.396	0.74 ± 0.04	−0.25
175	15.0 ± 0.3	2.411	2.50 ± 0.07	0.815	0.34 ± 0.04	−0.97

TABLE 2: (Continued)

	C_2H_6/A572					
	$n_1 = 0.318 \pm 0.005$ $-\Delta H_1 = 10.2 \pm 0.4$		$n_2 = 1.42 \pm 0.03$ $-\Delta H_2 = 8.1 \pm 0.2$		$n_3 = 3.7 \pm 0.3$ $-\Delta H_3 = 6.8 \pm 0.2$	
T (°C)	K_1	$-\Delta G_1$	K_2	$-\Delta G_2$	K_3	$-\Delta G_3$
40	176.7 ± 0.6	3.2186	15.0 ± 0.1	1.683	1.35 ± 0.05	0.185
55	74 ± 1	2.81	7.6 ± 0.2	1.33	0.75 ± 0.08	−0.19
70	42.0 ± 0.4	2.548	4.81 ± 0.09	1.072	0.53 ± 0.03	−0.43
100	13.9 ± 0.3	1.949	1.88 ± 0.07	0.466	0.23 ± 0.03	−1.08

[a] Process capacities given in mmol·g^{-1}. [b] Enthalpies of interaction given in kcal·mol^{-1}. [c] Free energies of interaction given in kcal·mol^{-1}.

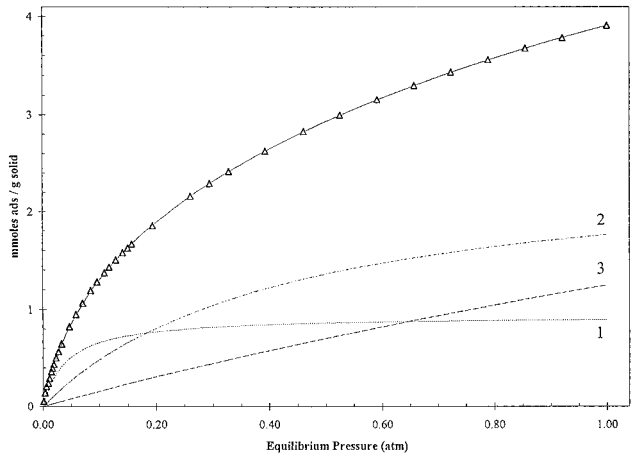

Figure 2. Process resolved adsorption for CH_4 by A572 at −43 °C. The points represent the experimental adsorption values and the solid line calculated values. The component isotherms, labeled 1, 2, and 3 for processes 1−3, are calculated using the n and K values from Table 2 with eq 3.

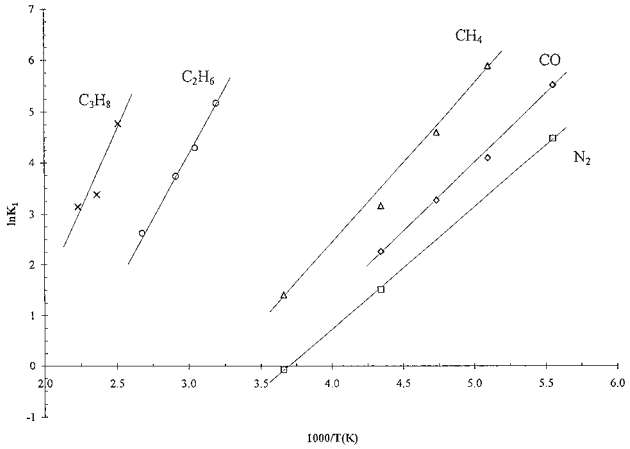

Figure 3. ln K_1 vs $1/T$ plots for the studied adsorptives by A572.

constants, K_i, describe the extent of occupancy at a specified external pressure. Since N_2, CO, CH_4, C_2H_6, and C_3H_8 adsorptions were measured above their respective critical temperatures, condensation in the pores is avoided and only solid−probe interactions are expected. Bilayer interactions would occur only if the surface is filled or if the magnitude of K_{bilayer} is comparable to K_i. Each K_i can be an average value that includes a range of K's so close in magnitude that they cannot be resolved further within the experimental accuracy.

It is possible to calculate the contribution of each process to the total isotherm by substituting the set of n_i's and K_i's into eq 3. Figure 2 shows the process-resolved adsorption of CH_4 by A572 at −43 °C. At moderate pressures, several adsorption processes occur simultaneously. At ∼1 atm, process 1 is essentially complete, process 2 is ∼70% complete, and process 3 has ∼75% of its capacity remaining. For the accurate determination of the two unknowns for each process, n_i and K_i, the process must be at least 60% complete.[27] In this study of methane, the process 1 and 2 parameters are the most accurately known. If a more accurate determination of the process 3 parameters were desired, studies at either higher equilibrium pressures or lower temperatures is required.

For those adsorptives in Table 2 that have large errors in K_3 and n_3, the amount adsorbed is far from filling the pore 3 capacity, resulting in a poor definition of the parameters. The degree of saturation for a process is reflected in the slope in the isotherm of the resolved process with an appreciable slope, suggesting that saturation is not complete. Large errors for some of the K_1 values are attributed to completion of process 1 before a significant number of data points can be taken to define the process. If improved accuracy of these K values is needed, data at lower equilibrium pressures or higher temperatures where less adsorptive is taken up is required.

Adsorptive Affinities. The adsorption equilibrium constant, K_i, quantifies the extent of adsorption of a given adsorptive by a solid. The magnitude of K depends on both the properties of the adsorptive and the solid. The observed linearity of the ln K_i vs T^{-1} plots, Figure 3, leads to the enthalpies of adsorption, ΔH_i, summarized in Table 2. The enthalpy values measure the strength of the adsorbate−adsorbent interaction while the equilibrium constants have both enthalpic and entropic contributions.

A plot of ΔH_1 for adsorption by A572 vs adsorptive polarizability for N_2, CO, CH_4, C_2H_6, and C_3H_8 shows a linear correlation. It is significant that this plot is linear for N_2, CO, CH_4, C_2H_6, and C_3H_8 given that these adsorptives have different sizes and therefore utilize different size pores for process 1. Similar correlations exist for processes 2 and 3. This result enables us to conclude that, in all cases, a given adsorptive selects appropriate pores from the distribution available in the solid that enable it to interact with the pore walls in the same manner for a given process.

The slope of the line on the polarizability plot characterizes the solid in terms of an effective polarizability for the group of pores involved in the process. Deviations of polar gas molecules from the polarizability plot can be used to further characterize the solid. If these deviations arise from nonspecific interactions, the magnitude of the deviation can be correlated to the dipole moment or to other measures of adsorptive polarity. The slope of the line for a plot of the deviations vs adsorptive polarity is a constant characterizing the solid polarity. If the deviations arise because of specific donor−acceptor interactions, attempts can be made to characterize the surface donor or acceptor strength by fitting the deviations to the E and C model.[28] The limited data available at present does not permit this further characterization of the surface properties of A572 and PPAN and the above discussion is presented to show the potential of this model.

As shown in Figure 4, there is a linear relationship between the square root of the van der Waals constant, a, and the

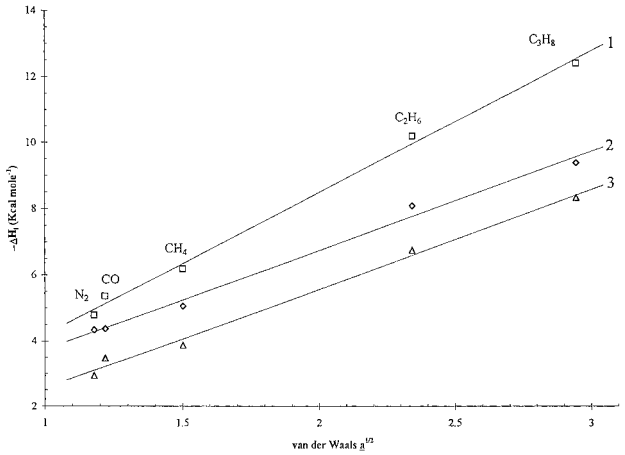

Figure 4. Correlations of the enthalpies of adsorption with the square root of the van der Waals *a* constant for the adsorptive. Process 1 is represented by □, with ◇ and △ representing processes 2 and 3, respectively. The equations for the best fit lines along with the associated R^2 values for processes 1−3 are given as follows: $y = 4.30x - 0.101$, $R^2 = 0.996$; $y = 3.00x + 0.751$, $R^2 = 0.992$; $y = 3.01x - 0.454$, $R^2 = 0.993$.

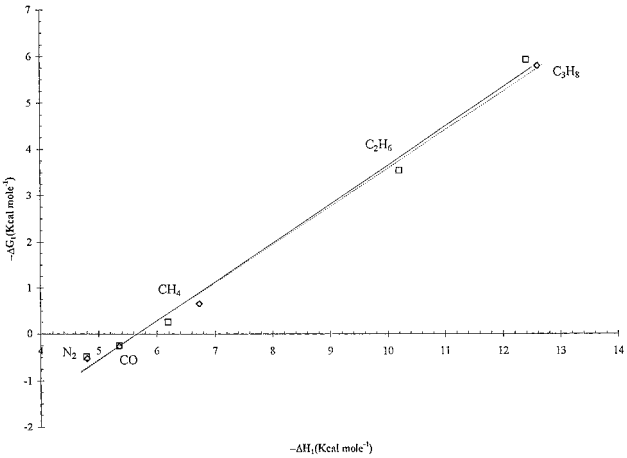

Figure 5. Correlation of the enthalpies of adsorption with the free energies of adsorption calculated at 25 °C. The adsorptives are shown for process 1 on A572, □, and PPAN, ◇. The equations for the best fit lines along with the associated R^2 values for process A572 and PPAN are given as follows: $y = 0.842x - 4.76$, $R^2 = 0.993$; $y = 0.826x + 4.67$, $R^2 = 0.997$.

enthalpy of interaction of the adsorptive with the solid PPAN. As *a* increases, the attractive forces between gas molecules increase. These attractive forces in the gas parallel nonspecific interactions of the gas with the solid and provide the driving force for adsorption. All of the adsorptives investigated with A572 and PPAN fall on or near the best fit line. We conclude that the solid-adsorptive interactions are nonspecific interactions. The good fit of the adsorption data for the lowest measured pressure to K_1 suggests that if any strong donor−acceptor sites are present they must be at concentrations, per gram of solid, considerably less than the number of moles of gas adsorbed for this lowest pressure measurement.

For many applications of porous solids, the equilibrium constants for the various processes are of prime concern. Figure 5 shows the linear relationship between $-\Delta G$ and $-\Delta H$ for process 1 and 2 on PPAN and A572. Thus, the free energies correlate to polarizability and the van der Waals *a* parameter in the same manner as $-\Delta H$. The plot of $-\Delta G$ for A572 vs the van der Waals *a* parameter is shown in Figure 6. These plots have practical utility for the prediction of $-\Delta G$ and thus process

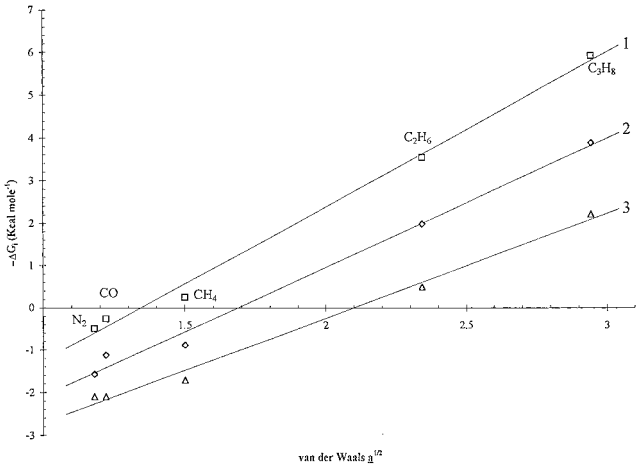

Figure 6. The free energies of adsorption on A572 at 25 °C vs the square root of the van der Waals *a* constant for each adsorptive. Process 1 is represented by □, with ◇ and △ representing processes 2 and 3, respectively. The equations for the best fit lines along with the associated R^2 values for processes 1−3 are given as follows: $y = 3.63x - 4.87$, $R^2 = 0.995$; $y = 3.04x + 5.13$, $R^2 = 0.991$; $y = 2.47x - 5.18$, $R^2 = 0.992$.

TABLE 3: Process Resolved Pore Volumes and Surface Areas

	A572			PPAN		
process	mmol ads	mL ads	area (m^2 g^{-1})	mmol ads	mL ads	area (m^2 g^{-1})
		N_2			N_2	
1	0.463	0.016	45	0.499	0.018	49
2	1.790	0.063	175	1.588	0.056	155
3	5.335	0.189	520	3.585	0.127	350
total	7.588	0.269	740	5.672	0.201	553
		CO			CO	
1	0.520	0.018	47	0.570	0.020	51
2	1.898	0.066	171	1.802	0.063	163
3	4.932	0.172	445	3.642	0.127	329
total	7.351	0.257	664	6.014	0.210	543
		CH_4			CH_4	
1	0.938	0.035	100	0.285	0.011	31
2	2.492	0.094	267	1.401	0.053	150
3	5.394	0.204	578	3.628	0.137	389
total	8.824	0.334	945	5.314	0.201	569
		C_3H_8			C_3H_8	
1	0.198	0.015	43	0.221	0.017	48
2	1.007	0.075	219	0.874	0.066	190
3	2.488	0.187	541	1.529	0.115	332
total	3.693	0.277	803	2.624	0.197	570
		C_2H_6				
1	0.318	0.017	44			
2	1.422	0.075	197			
3	3.718	0.196	515			
total	5.459	0.287	756			

equilibrium constants for adsorption of gas molecules by these solids.

Process Capacities. In addition to the above insights from the multiple equilibrium model, the n_i values reflect the capacity of pores in a particular size regime. When combined with the molar volume of the adsorptive in its liquid state, the n_i's can be converted to process accessible pore volumes. This assumes that gas molecules of the adsorbed phase pack as effectively on the solid as they do in the liquid. The process resolved pore volumes are given in Table 3. Summing the capacities for N_2 adsorption by A572 for all three processes results in a volume of 0.269 mL·g^{-1}. A similar result, 0.257 mL·g^{-1} is obtained from the analysis of the CO data. These quantities are smaller than the 0.43 mL micropore volume that standard N_2 porosimetry claims to be micropores. The observed three-process

adsorption for these gases is occurring exclusively in the smaller <8 Å micropore region which is now resolved into different pore size regimes.

A comparison of the *n*'s for processes 1 and 2 for N_2 and CO adsorption by A572 shows that there is more capacity for CO. Process 1 capacity can be accounted for by the slightly smaller molar volume of CO that allows it to access smaller pores than N_2. The greater process 2 capacity for CO vs N_2 shows that the slight polarity of the CO molecule enables it to utilize slightly larger pores than N_2 in process 2.

Similar conclusions may be drawn for N_2 and CO adsorption by PPAN. Again, the 0.201 and 0.210 mL·g^{-1} capacities for N_2 and CO, respectively, show that only ∼60% of the 0.33 mL·g^{-1} H-J micropore volume is being utilized by these adsorptives. PPAN process 1 capacities for N_2 and CO are larger than for A572 showing that PPAN has a greater number of these smaller micropores. PPAN also utilizes more of its total micropore volume for N_2 and CO process 1 adsorption, ∼6%, than does A572 at <4%. The greatest difference between these two adsorbents in terms of N_2 and CO adsorption is reflected in the process 3 capacities with A572 having a greater number of pores that accommodate this type of adsorption.

The total C_3H_8 capacity for processes 1−3 is 0.28 mL·g^{-1} for A572 and 0.20 mL·g^{-1} for PPAN corresponding to 65 and 60% of the total H-J micropore volumes. The adsorptive C_3H_8 is larger than CH_4 and cannot utilize the same process 1 micropores. The process 1 pores for C_3H_8 are mainly the process 2 pores of N_2 and CO as well as the smaller process 3 pores of N_2. Process 2 for C_3H_8 occurs in the process 3 pores of N_2, while process 3 for C_3H_8 utilizes the remaining micropores. The total volume of A572 utilized for processes 1−3 for C_3H_8 is 0.28 mL. With the smaller 0.02 mL of small micropores inaccessible, the volume of C_3H_8 adsorbed for the three processes corresponds to ∼75% of the remaining micropore volume. Comparison with methane suggests that 0.05 mL·g^{-1} of small pores accessed by methane is not accessed by propane.

The adsorptives N_2 and CO suggest that A572 has a group of smallest pores, component I, with ∼0.02 mL·g^{-1} capacity. A second group of slightly larger pores, component II, has a capacity of 0.06 mL·g^{-1}. The next larger group, component III, has a capacity of 0.18 mL·g^{-1}. The methane capacities require an additional 0.07 mL·g^{-1} component IV capacity. The 0.33 mL·g^{-1} total pore volume is adequate to accommodate all of the ethane and propane adsorbed with the lower total adsorption, indicating that some of the smaller pores are not accessed by these adsorptives. PPAN has a group of smallest pores (I) with ∼0.02 mL·g^{-1} capacity that do not adsorb methane, and a second group (II) with ∼0.06 mL·g^{-1} capacity that corresponds to process 2 for CO and N_2 as well as process 1 and 2 for methane. A third group (III) at 0.13 mL·g^{-1} corresponds to process 3 for CO and N_2 and most of process 3 for methane. The volume of propane adsorbed can be accommodated in the group II and III pores, suggesting a more narrow pore distribution for PPAN PPAN has small pores that even methane does not access, but has a lower volume for component III pores than does A572.

The surface areas corresponding to the above groups of pores can be calculated by multiplying the millimoles of gas adsorbed by the adsorptive cross-sectional area[29] per millimole. Since multilayer formation does not occur, this quantity provides a better estimate of the solid surface area than BET. The MEA area corresponds to area available in the pores of 8 Å or less diameter but these pores are the only ones accessed by these adsorptives at these temperatures and pressures. Table 3 contains the surface areas that would result if a monomolecular film of the adsorptive formed on the solid for each of the three processes. Note that the surface areas, like the pore volumes, are adsorptive dependent.

Utility of Multiple Equilibrium Parameters The multiple equilibrium model leads to two important kinds of fundamental information for characterizing porous solids. The data permit comparisons of the affinity of a solid for different adsorptives and determining capacities for pore distributions. The relationships shown in Figure 5 should permit the estimation of K_1 for any small molecule whose van der Waals *a* parameter is known. In using these carbonaceous adsorbents to separate mixtures of these gases, the best separation will be achieved for adsorptives with a large difference in *K*.

The data are also of use in adsorbent selection. First, consider CH_4 as the adsorptive. It is a nonpolar, nonreactive, and noncondensible gas at the temperatures and pressures studied. Process 1 has a larger capacity, but smaller *K* for A572 than PPAN. Thus, if CH_4 needed to be removed from a dilute gas, PPAN would be a more effective material, but would have a lower total capacity. If the solids were compared for storage and transport of CH_4, the results indicate that A572 has much more capacity and would be a better choice than PPAN at 1 atm external pressure. However, the larger 45% of the 15−20 Å pores, the mesopores, or the macropores of A572 are not utilized. Thus, our analysis of the micropore distribution suggests that a modification in the design of the solid's pore distribution will produce a more desirable material for this application.

We are in a position to predict the adsorption isotherm of any adsorptive that has molecular dimensions comparable to the adsorptives studied. This would be accomplished by assuming comparable pore volumes for the two adsorptives in the three processes and converting these to *n* values for the new adsorptive using its molar volume. The *K*'s for the three processes can be estimated from the van der Waals plot. Substituting these *K*'s and *n*'s into eq 3 produces the predicted adsorption isotherm for any given temperature above the critical temperature.

Effective Pressure. For heterogeneous catalytic processes, the ability of the porous support to concentrate reactants around the catalytic center can lead to an increase in reaction rates. In a homogeneous gas phase reaction, the concentration is increased by increasing the pressure. The concentrating effect of porosity can be illustrated by calculating an effective pressure, P_{eff}, that would have to be applied to an ideal gas to obtain a similar concentration to that in the pore for an equal number of moles of gas. Since the number of moles of gas adsorbed varies with the pressure of gas over the solid and the temperature as well as the adsorbent, P_{eff} is calculated for illustrative purposes at an external pressure of 1.0 atm and ambient temperature. Other temperatures and pressures can be used depending upon the desired application. P_{eff} provides a facile comparison of the concentrating power of solid supports. Using the ideal gas law, the number of moles adsorbed, and the total micropore volume of the solid, eq 4 is used to calculate P_{eff}.

$$P_{\text{eff}} = n_{\text{tot}}RT/V_{\mu\text{pore}} \tag{4}$$

This quantity represents the pressure that would have to be exerted on an ideal gas in a container whose volume corresponds to the volume of the micropores in order to obtain a comparable concentration of gas. By using the total micropore volume, we are in effect assuming that processes 1, 2, and 3 provide a reactant reservoir for catalysis in all the micropores. For many reasons, P_{eff}, is a semiquantitative concept, e.g., a gas under

TABLE 4: P_{eff} Values

solid	adsorptive	mmols ads[a]	P_{eff}
A572	N_2	0.408	23.2
	CO	0.594	33.8
	CH_4	1.316	74.9
	C_2H_6	4.284	243.8
	C_3H_8	3.633	206.7
PPAN	N_2	0.384	28.5
	CO	0.532	39.4
	CH_4	1.042	77.3
	C_3H_8	2.589	191.9

[a] Calculated mmoles adsorbed at 25 °C and 1 atm.

these conditions would not be ideal, and the adsorptive is distributed over several adsorption processes. The utility of this quantity is to provide a dramatic comparison of the influence of porosity on reactivity by expressing the influence of porosity in terms of the more widely appreciated influence of pressure on the reactivity of a homogeneous gas phase reaction. The influence would be even greater than P_{eff} indicates for applications involving only the process 1 or process 1 and 2 pores.

Table 4 summarizes the number of moles of various gases adsorbed at an equilibrium pressure of 1.0 atm, and the calculated P_{eff}, for all of the isotherms measured for PPAN and A572. These gases cannot be liquefied at any effective pressure given the temperature involved. These materials approach concentrations corresponding to reactions in the liquid, and the pressure generated by the solid's porosity can be assumed to be greater than the partial pressure of the liquid adsorptive.

The utilization of the data in Table 4 for catalytic reactions can be illustrated. Consider a reaction of CH_4 that requires an external pressure of 50 atm in order to occur in a gas phase homogeneous reaction at room temperature. If PPAN is the catalyst, with active sites in the micropores, the reaction can be carried out at 1 atm external pressure and at a higher CH_4 concentration attained in the PPAN catalyst than in the gas phase at 50 atm. If a catalyst is added, the micropore volume and the moles of gas adsorbed by the supported catalyst would have to be recalculated to determine the effective pressure.

If the P_{eff} indicates that one of the reactants is present as a liquid in the pores, and that the other is a gas, the reaction in the porous solid is comparable to carrying out a liquid−gas reaction. If condensation of the liquid reactant prevents transport of the gaseous reactant to the catalyst, the reaction will be slowed. If the reaction product is adsorbed more effectively than the reactants, product inhibition will occur. These considerations suggest that high surface area, which often parallels high porosity, does not provide a complete picture of catalytic reactivity. The information from equilibrium analyses has the potential to lead to advances in understanding of heterogeneous catalysis and a rational basis for support selection.

Conclusions

Adsorption curves as a function of pressure at multiple temperatures support a three-process equilibrium model for the two carbonaceous adsorbents A572 and PPAN. Comparison of the volume of gas adsorbed with the pore volume from H-J t-plots and BJH analyses indicates that the three processes are occurring in the micropores. Process 1 is occurring in micropores of molecular dimensions, process 2 in micropores slightly larger than molecular dimensions, and process 3 in micropores up to two molecular dimensions. Thus, this approach resolves the micropore volume into smaller components. The surface areas for N_2, CO, CH_4, C_2H_6, and C_3H_8 provide values corresponding to a monomolecular coverage because the studies are carried out above the critical temperature. As expected for a monolayer, the resulting process enthalpies are well above the enthalpies of vaporization. Surface areas are adsorptive and process dependent. It is anticipated that this added detail concerning surface areas will be of value in practical applications, particularly those that utilize only certain pores.

The model provides free energies and enthalpies for the different adsorptives in each of the three interpreted adsorption processes. These results correlate with the polarizabilities of nonpolar molecules and the correlations indicate a comparable surface polarizability for A572 and PPAN. These correlations enable one to predict the relative affinities of adsorptives whose polarizabilities or van der Waals constants are known and lead to a procedure whereby the adsorption isotherm of gas adsorptives can be predicted.

In addition to the adsorption equilibrium constant, the effective pressure, is proposed to indicate the ability of solid supports to concentrate gases in catalytic systems. In the area of catalysis, high surface area is normally desired in order to get the greatest amount of catalyst in the smallest volume. The concentrating effects of highly porous supports add a second favorable factor to consider in the use of solid materials as catalyst supports.

Acknowledgment. This work was supported by Rohm and Haas and ERDEC/ARO. The authors thank Dr. Phil L. Rose for his donation of samples of PPAN and Dr. Bill Brendley for samples of A572 carbonaceous adsorbents. Helpful comments from Dr. Bill Brendley and Steve Maroldo are also acknowledged.

References and Notes

(1) Langmuir, I. *J. Am. Chem. Soc.* **1918**, *40*, 1361.
(2) Ruthven, D. M. *Principles of Adsorption and Adsorption Processes*; John Wiley and Sons: New York, 1984.
(3) Sing, K. S. W.; Everett, D. H.; Haul, R. A. W.; Moscou, L.; Pierotti, R. A.; Rouquerol, J.; Siemieniewska, T. *Pure Appl. Chem.* **1985**, *57*, 603.
(4) Rouquerol, J.; Avnir, D.; Fairbridge, C. W.; Everett, D. H.; Haynes, J. H.; Pernicone, N.; Ramsay, J. D. F.; Sing, K. S. W.; Unger, K. K. *Pure Appl. Chem.* **1994**, *66*, 1739.
(5) Everett, D. H. *Langmuir* **1993**, *9*, 2586.
(6) Sing, K. S. W. *Carbon* **1989**, *27*, 5.
(7) Stoeckli, H. F. *Carbon* **1990**, *28*, 1.
(8) Jagiello, J.; Bandosz, T. J.; Schwarz, J. A. *Langmuir* **1996**, *11*, 1744.
(9) Aharoni, C.; Romm, F. *Langmuir* **1995**, *11*, 1744.
(10) Jaroniec, M.; Gadkaree, K. P., Choma, J. *Colloids Surf. A* **1996**, *118*, 203.
(11) Heuchel, M.; Jaroniec, M. *Langmuir* **1995**, *11*, 4532.
(12) Chen, S. G.; Yang, R. T. *Langmuir* **1994**, *10*, 4244.
(13) Aranovich, G. L.; Donohue, M. D. *Carbon* **1995**, *33*, 1369.
(14) Ross. S.; Morrison, I. D. *Surf. Sci.* **1975**, *52*, 103.
(15) Everett, D. H.; Powl, J. C. *J. Chem. Soc., Faraday Trans. 1* **1976**, *72*, 619.
(16) Drago, R. S.; Burns, D. S.; Lafrenz, T. J. *J. Phys. Chem.* **1996**, *100*, 1718.
(17) Brunauer, S.; Emmett, P. H.; Teller, E. *J. Am. Chem. Soc.* **1938**, *60*, 309.
(18) Harkins, W. D.; Jura, G. *J. Am. Chem. Soc.* **1944**, *66*, 1366.
(19) Barrett, E. P.; Joyner, L. G.; Halenda, P. P. *J. Am. Chem. Soc.* **1951**, *73*, 373.
(20) Gordon, A. J.; Ford, R. A. *The Chemist's Companion*; John Wiley and Sons: New York, 1972; p 451.
(21) Deming, S. N.; Morgan, S. L. *Anal. Chem.* **1973**, *45*, 2784.
(22) Leggett, D. J. *J. Chem. Educ.* **1983**, *60*, 707.
(23) Neely, J. W. *Carbonaceous Adsorbents for the Treatment of Ground and Surface Waters*; Marcel Dekker: New York, 1982.
(24) PPAN is a proprietary, high surface area, pyrolyzed poly(acrylonitrile) product supplied by Rohm and Haas Co.
(25) Jenkins, G. M.: Kawamura, K. *Polymeric Carbons−Carbon Fibre, Glass, and Chemistry*; Cambridge University Press: London, 1976.
(26) Lafyatis, D. S.; Tung, J.; Foley, H. C. *Ind. Eng. Chem. Res.* **1991**, *30*, 865.
(27) Person, W. B. *J. Am. Chem. Soc.* **1965**, *87*, 167.
(28) Drago, R. S. *Applications of Electrostatic−Covalent Models in Chemistry*; Surfside Scientific Publishers: Gainesville, FL, 1994.
(29) McClellan, A. L.; Harnsberger, H. F. *J. Colloid Interface Sci.* **1967**, *23*, 577.